CellPress

Developmental Cell
Article

Redox Regulation by Pitx2 and Pitx3 Is Critical for Fetal Myogenesis

Aurore L'honoré,[1,*] Pierre-Henri Commère,[2] Jean-François Ouimette,[3,5] Didier Montarras,[1] Jacques Drouin,[3,4] and Margaret Buckingham[1,4]

[1]Department of Developmental and Stem Cell Biology, CNRS URA 2578, 28 rue du Dr Roux, 75015 Paris, France
[2]Platform of Cytometry, Institut Pasteur, 28 rue du Dr Roux, 75015 Paris, France
[3]Laboratory of Molecular Genetics, Institut de Recherches Cliniques de Montréal, Montréal, QC H2W 1R7, Canada
[4]Co-senior author
[5]Present address: UMR 7216 Epigenetics and Cell Fate Unit, Université Paris Diderot, 35 rue Hélène Brion, 75013 Paris, France
*Correspondence: aurore.lhonore@pasteur.fr
http://dx.doi.org/10.1016/j.devcel.2014.04.006

SUMMARY

During development, major metabolic changes occur as cells become more specialized within a lineage. In the case of skeletal muscle, differentiation is accompanied by a switch from a glycolytic proliferative progenitor state to an oxidative postmitotic differentiated state. Such changes require extensive mitochondrial biogenesis leading to increased reactive oxygen species (ROS) production that needs to be balanced by an antioxidant system. Our analysis of double conditional *Pitx2/3* mouse mutants, both in vivo during fetal myogenesis and ex vivo in primary muscle cell cultures, reveals excessive upregulation of ROS levels leading to DNA damage and apoptosis of differentiating cells. This is a consequence of downregulation of *Nrf1* and genes for antioxidant enzymes, direct targets of Pitx2/3, leading to decreased expression of antioxidant enzymes, as well as impairment of mitochondrial function. Our analysis identifies Pitx2 and Pitx3 as key regulators of the intracellular redox state preventing DNA damage as cells undergo differentiation.

INTRODUCTION

Tissue formation during development depends on tightly regulated steps of progenitor cell self-renewal, transitory amplification of tissue-specific precursor cells, and their subsequent differentiation. The dynamic phenotypic changes that cells undergo during this process include major metabolic adaptation, as exemplified by skeletal muscle. Myogenic progenitors are characterized by the expression of Pax3 and Pax7, which are required both for maintenance of this stem cell population (Relaix et al., 2005) and for activation of *Myf5* and *MyoD*, which control entry into the skeletal muscle program (Davis et al., 1987; Weintraub et al., 1991). On activation of these myogenic determination genes, myoblasts proliferate before exiting the cell cycle, activating the myogenic differentiation gene, *Myogenin*, and forming multinucleated differentiated muscle fibers. Gene regulatory networks for both transcription factors and signaling pathways involved in myogenesis have been partially identified (Buckingham and Vincent 2009); however, important aspects of the myogenic context that affect cell behavior remain obscure. This is the case for the control of reactive oxygen species (ROS) that are produced by oxidative phosphorylation when cells switch from a glycolytic proliferative progenitor state to an oxidative postmitotic differentiated state (Remels et al., 2010; Blanchet et al., 2011). The management of these by-products is critical as they can lead to oxidative stress and cell damage. In general, the control of ROS levels and of metabolic status is emerging as an important facet of stem cell biology, as illustrated by recent results on hematopoietic stem cells (Owusu-Ansah and Banerjee 2009; Takubo et al., 2010). ROS levels were shown to increase at the onset of differentiation in immortalized muscle cell lines (Malinska et al., 2012; Lee et al., 2011), but it is not clear whether this has functional significance in vivo or how it is regulated. *Pitx2* and *Pitx3*, two genes expressed in muscle progenitor cells, have been associated in lens and retina with glaucoma and cataracts (Amendt et al., 1998; Semina et al., 1996, 1997), two disorders that involve oxidative stress (Babizhayev, 2012). During myogenic development, these two genes lie downstream of *Pax3/7* (Lagha et al., 2010; L'honoré et al., 2010) and upstream of the myogenic factor genes. While Pitx2 decreases at the onset of differentiation, Pitx3 is maintained in terminally differentiated cells. In *Pitx3* mutants, muscle development is not notably perturbed. *Pitx2* transcription, which is normally downregulated, is maintained in the absence of Pitx3, thus providing compensation (L'Honoré et al., 2007).

In this report, we have investigated the roles of Pitx2 and Pitx3 during fetal myogenesis. Both in vivo by examining the muscle phenotypes of conditional *Pitx2/Pitx3* double mutants and ex vivo in primary myogenic cell cultures, we observed a deficit in skeletal muscle due to cell death of myogenic cells at the onset of differentiation. We found an essential role for Pitx2 and Pitx3 in the management of ROS during the transition from proliferation to differentiation. In the absence of both Pitx factors, differentiating myoblasts accumulate abnormally high levels of ROS, leading to irreversible DNA damage and apoptosis. We demonstrate that this excessive level is largely due to deficient expression of the transcription factor nuclear respiratory factor 1 (Nrf1) and of its target genes implicated in mitochondrial respiration and in the antioxidant pathway. Using in vivo chromatin immunoprecipitation (ChIP),

we show that Pitx2 and Pitx3 are direct regulators of both *Nrf1* and its antioxidant targets, demonstrating two levels of ROS regulation by these transcription factors.

RESULTS

Absence of Pitx2/3 Impairs Skeletal Muscle Development

In view of the apparent compensation of Pitx3 deficiency by Pitx2, we evaluated the involvement of both factors in fetal myogenesis using *Pitx2:Pitx3* double conditional mutants. In contrast to embryonic myogenesis when only Pitx2 is expressed in Pax3-positive progenitors (L'Honoré et al., 2007), during fetal myogenesis, both Pitx2 and Pitx3 are present in progenitors labeled by Pax7 (Figures S1A–S1F and S1M available online), and early differentiating cells marked by Myogenin (Figures S1G–S1L), before subsequent downregulation of *Pitx2* in differentiated cells (L'Honoré et al., 2007). In order to delete conditional alleles of these genes prior to the onset of myogenesis, we used the transgenic *MSD-cre* line, in which Cre recombinase is expressed throughout the paraxial mesoderm (Beckers et al., 2000), or for differentiated muscle, an *HSA-cre* line where the human skeletal actin (HSA) promoter directs *Cre* expression (Miniou et al., 1999). Using the conditional reporter alleles $R26R^{mTomato\text{-}STOP\text{-}mGFP}$ and $R26R^{nLacZ}$, we confirmed the robust expression of the reporter gene in the myogenic lineage of the trunk and limbs in these *Cre* lines (Figures S1N and S1O) and the effective loss of Pitx2/3 expression (Figure S1P). $Pitx2^{flox/flox}$:$Pitx3^{-/flox}$:*MSD-cre* mutants die at birth and can be easily distinguished from their littermates. They are smaller, display a bent posture, and have an enlarged abdomen compared to controls. This phenotype is already observed at embryonic day (E)15.5 (Figures S1Q and S1R) and is suggestive of inadequate development of the musculature, especially in the trunk (Grifone et al., 2005). To analyze the consequences of deletion of *Pitx2/3* genes, we first examined the development of trunk and limb skeletal muscles at E13.5 in the presence of the *MSD-cre* transgene. Whole-mount in situ hybridization with a *Myogenin* probe showed a striking reduction in skeletal muscle in the body (Figures 1A and 1B). As this reduction was not equal in all muscles, and to check the activity of the *MSD-cre* transgene, we performed the Pitx2 and Pitx3 deletion using the $Pax3^{cre/+}$ line. *Myogenin* expression of $Pitx2^{flox/flox}$:$Pitx3^{-/flox}$:$Pax3^{cre/+}$ embryos at E13.5 (Figures S1S and S1T) displayed a pattern similar to that of $Pitx2^{flox/flox}$:$Pitx3^{-/flox}$:*MSD-cre* mutants, demonstrating variable sensitivity of different muscles to the absence of Pitx2/3. In view of the coexpression of the two *Pitx2/3* genes in progenitor cells and early differentiating cells, we then examined potential defects at both stages that might lead to the impairment in mutant muscle differentiation. Using TUNEL immunofluorescence staining, we observed a major increase in apoptosis in developing skeletal muscle in E12.5 mutant embryos crossed with the *MSD-cre* line (Figures 1F–1H, 1L, and 1M), compared to control embryos (Figures 1C–1E and 1M). Such cell death is first detected at E11.5 (data not shown) and still observed in mutant embryos later during development at E16.5 (Figures 1N and 1O). We did not find any significant difference in the number of Pax7-positive progenitor cells in mutant versus control embryos at E13.5 (Figure S1U) and at E16.5 (data not shown), suggesting that the absence of Pitx2 and Pitx3 does not affect the proliferation or survival of Pax7-positive myogenic progenitors. Consistent with this, we did not detect an increased number of Pax7/TUNEL double-positive cells in mutant embryos compared to controls (Figures 1C, 1F, and 1L). However, we observed that a large proportion of cells that were undergoing apoptosis were also marked by Myogenin (61%) and MF20 (42%) expression (Figures 1G, 1H, and 1L). We then examined the consequences of impaired expression of Pitx2 and Pitx3 in differentiated cells and did not detect any significant apoptosis in muscle masses of $Pitx2^{flox/flox}$:$Pitx3^{-/flox}$:*HSA-Cre* mutants either at E12.5 (Figures 1I–1K and 1M) or E16.5 (Figure 1P). Altogether, these data demonstrate that loss of *Pitx2/3* gene expression in the myogenic lineage leads to impaired myogenesis due to apoptosis of cells at the onset of differentiation.

Ex Vivo Deletion of *Pitx2* and *Pitx3* in Fetal Muscle Progenitors Results in Apoptosis of Differentiating Myoblasts, Leading to Defective Myogenesis

To explore the mechanism by which the absence of Pitx2/3 affects muscle cell survival, we next carried out conditional ablation of both genes in primary cultures of myogenic progenitors isolated from fetal muscle. We generated $Pitx2^{flox/flox}$:$Pitx3^{-/flox}$:$R26R^{cre\text{-}ERT2/+}$:$Pax3^{GFP/+}$ embryos, which facilitated the direct isolation of Pax3(GFP)-positive muscle progenitor cells by flow cytometry (Montarras et al., 2005; Figure S2A). We first validated the myogenic identity of green fluorescent protein (GFP)-sorted cells isolated from $Pax3^{GFP/+}$ embryos and confirmed that more than 98% of the cells expressed MyoD after 48 hr in culture (Figure S2B). Using immunocytochemistry with an antibody that recognizes both Pitx2 and Pitx3, and antibodies to MyoD, Myogenin, P21, and Troponin T, we showed that the pattern of expression of Pitx2/3 ex vivo in control $Pax3^{GFP/+}$ cells (Figures S2C and S2D) is similar to what we had previously observed in vivo (Figures S1A–S1L). After addition of 4-hydroxytamoxifen (4-OHT) to the culture medium (Figure S2E), recombination of both *Pitx2* and *Pitx3* alleles was complete after 36 hr of culture (Figure S2F), leading to the complete absence of Pitx2/3 staining by immunocytochemistry at 48 hr (Figure S2G). We then investigated the consequences of *Pitx2/3* deletion on ex vivo myogenesis. Deletion of *Pitx2* and *Pitx3* genes affects expansion of the population (see DAPI in Figure 2A) and leads to defective differentiation marked morphologically by the absence of multinucleated myotubes after 120 hr of culture (Figure 2A, phase contrast), while 4-OHT treatment of control cells has no effect (Figure S2H). This phenotype is illustrated by the large reduction in Troponin T expression at 120 hr (Figures 2A and 2C). We then followed sequential expression of progenitor and differentiating cell markers. We did not detect any differences in the number of progenitors marked by expression of Pax7 (Figures S2I and S2K). Unlike the situation during embryonic myogenesis in the limb (L'honoré et al., 2010), MyoD is normally expressed in activated cells in the absence of Pitx2/3 (Figures S2I and S2K). The onset of differentiation occurs similarly in control and mutant cells, as shown by Myogenin expression at 72 hr (Figures 2B and 2C). However, by 96 hr, we observed a striking decrease (50%) in the mutant population compared to controls (Figures 2B and 2C). This decrease is essentially due to a reduction in the number of Myogenin-positive cells in the mutant cultures, while the

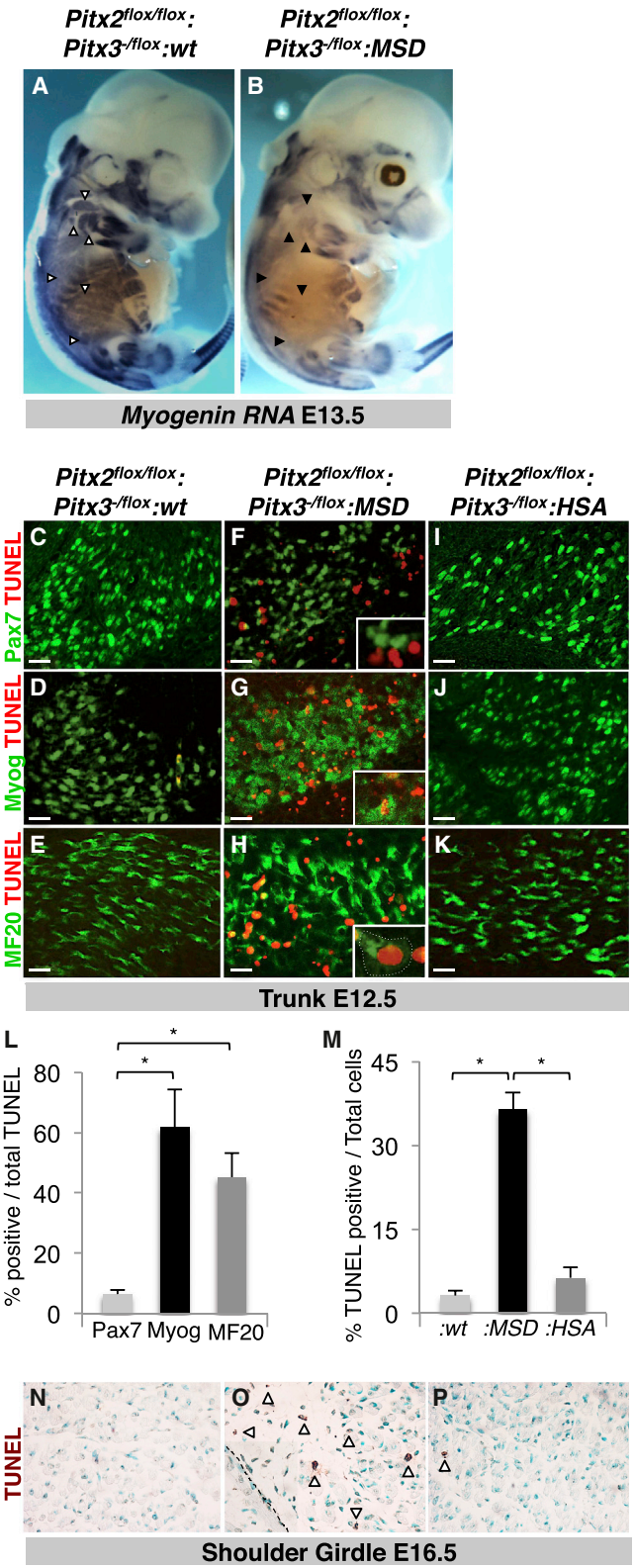

Figure 1. Inactivation of *Pitx2/3* Leads to Defective Differentiation during Fetal Myogenesis

(A and B) Whole-mount in situ hybridization with a probe for *Myogenin* RNA on (A) control *Pitx2*$^{flox/flox}$*:Pitx3*$^{-/flox}$*:wt* and (B) mutant *Pitx2*$^{flox/flox}$*:Pitx3*$^{-/flox}$*:MSD-cre* embryos at E13.5 shown in lateral views. Black arrowheads point to differences in expression. The experiments were performed with at least three embryos, and a representative picture of each genotype is shown.

(C–K) Coimmunohistochemistry on transverse sections of thoracic somites from (C–E) control *Pitx2*$^{flox/flox}$*:Pitx3*$^{-/flox}$*:wt*, (F–H) mutant *Pitx2*$^{flox/flox}$*:Pitx3*$^{-/flox}$*:MSD-cre*, and (I–K) mutant *Pitx2*$^{flox/flox}$*:Pitx3*$^{-/flox}$*:HSA-cre* embryos at E12.5 costained with the TUNEL reaction (red) and Pax7 (in C, F, and I); myogenin (Myog in D, G, and J), or muscle myosin heavy chain (MF20 in E, H, and K) antibodies. Scale bars, 20 μM.

(L) Quantification of the number of TUNEL-positive nuclei that express Pax7, Myogenin (Myog), or muscle Myosin Heavy Chain (MF20), shown as a percentage of the total TUNEL-positive population for mutant *Pitx2*$^{flox/flox}$*:Pitx3*$^{-/flox}$*:MSD-cre* embryos at E12.5 (n = 3 embryos, mean ± SD, *$p < 0.05$). Pax7/TUNEL-, Myogenin/TUNEL-, and MF20/TUNEL-positive nuclei were counted and expressed as a percentage of the total TUNEL-positive population.

(M) Quantification of the percentage of nuclei that are TUNEL positive for control *Pitx2*$^{flox/flox}$*:Pitx3*$^{-/flox}$*:wt* (:wt), mutant *Pitx2*$^{flox/flox}$*:Pitx3*$^{-/flox}$*:MSD-cre* (:MSD) and mutant *Pitx2*$^{flox/floc}$*:Pitx3*$^{-/flox}$*:HSA-cre* (:HSA) embryos at E12.5 (n = 3 embryos for each genotype; mean ± SD, *$p < 0.05$).

(N–P) Sagittal sections at shoulder level of E16.5 (N) control *Pitx2*$^{flox/flox}$*:Pitx3*$^{-/flox}$*:wt*, (O) mutant *Pitx2*$^{flox/flox}$*:Pitx3*$^{-/flox}$*:MSD-cre*, and (P) mutant *Pitx2*$^{flox/flox}$*:Pitx3*$^{-/flox}$*:HSA-cre* embryos stained for TUNEL activity. Open arrowheads point to examples of TUNEL-positive cells.

Myogenin-negative population is not affected (Figure 2C). This leads to an increased proportion of the *Pax7*-expressing cells in the population, as shown by reverse transcription followed by quantitative real-time PCR (qPCR) analysis of transcripts (Figure 2D).

We observed a severe increase in apoptosis in mutant cells compared to controls (Figures 2E and 2F), in agreement with in vivo results obtained with *Pitx2*$^{flox/flox}$*:Pitx3*$^{-/flox}$*:MSD-cre* mutants (Figures 1F–1H, 1L, and 1M). This apoptosis, marked by an increase of *p53* and *Noxa* expression (Figure 2G), is first detected at the onset of differentiation, at 72 hr, and is high after 96 hr of culture (Figure 2F). In keeping with what we observed in *Pitx2*$^{flox/flox}$*:Pitx3*$^{-/flox}$*:HSA-cre* mutants (Figures 1I–1K and 1M), deletion of *Pitx2/3* by the addition of 4-OHT at 72 hr did not affect the survival of differentiated cells (Figures 2E and 2F), with the same number of cells marked by Troponin T (Figures S2J and S2K).

Defects in cell cycle arrest at the onset of differentiation can lead to endoreplication of myotube nuclei and to their apoptosis (Zacksenhaus et al., 1996; Jiang et al., 2000). As *Pitx* genes have been implicated in upregulation of *p21* (Wei and Adelstein 2002; Cao et al., 2010), we investigated whether *Pitx2/3* mutant cells exit the cell cycle normally. At 72 hr, all Myogenin-positive cells were also marked by p21 expression in the presence or absence of Pitx2/3 (Figures S3A and S3B). Furthermore, mutant cells marked by Myogenin expression did not show increased 5-ethynyl 2′ deoxyuridine (EdU) incorporation compared to controls (Figures S3C and S3D), demonstrating that, in the absence of Pitx2 and Pitx3, cells cease DNA synthesis and exit the cell cycle normally at the onset of differentiation.

Pitx2/3 Mutant Cells Exhibit Abnormal ROS Levels, with Accumulation of DNA Damage during Differentiation, and Are Rescued by Antioxidants

Ex vivo deletion of *Pitx2/3* reproduced our in vivo results showing apoptosis of myogenic cells at the onset of differentiation.

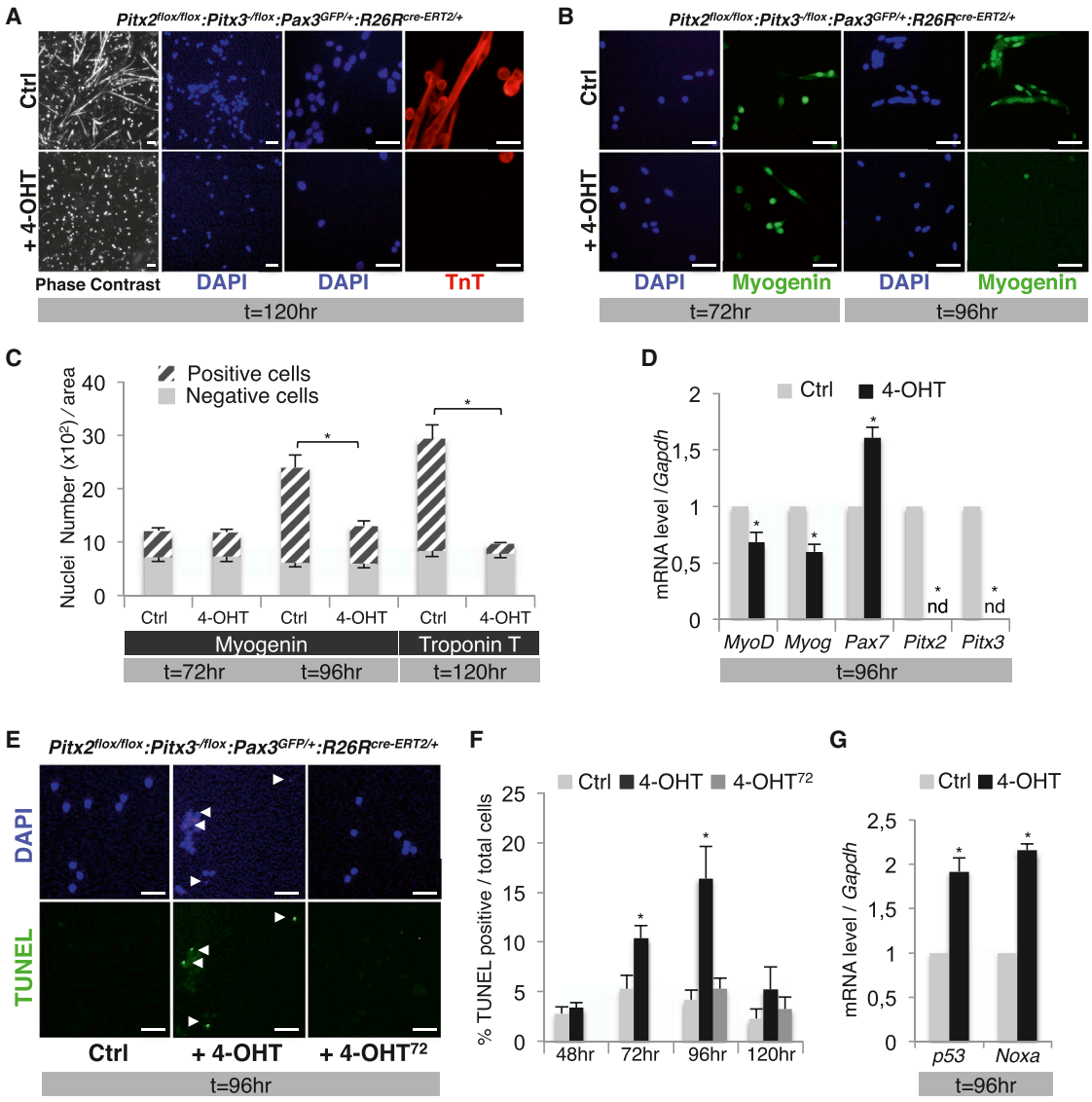

Figure 2. Ex Vivo Inactivation of *Pitx2/3* Leads to Defective Differentiation due to Apoptosis of Differentiating Myoblasts

(A–C) GFP-positive cells, isolated from inducible mutant *Pitx2*$^{flox/flox}$:*Pitx3*$^{-/flox}$:*Pax3*$^{GFP/+}$:*R26R*$^{Cre-ERT2/+}$ embryos at E13.5 were cultured (A) for 120 hr and (B) for 72 hr and 96 hr and in the presence or absence (Ctrl) of 0.5 μM 4-OHT. Cells were stained with DAPI and by immunocytochemistry with Myogenin (green) antibody at 72 hr and 96 hr in (B) and with Troponin T (TnT, red) antibody at 120 hr, with phase contrast images on the left in (A). Scale bars, 20 μM. (C) Results were quantified by counting positive and negative nuclei for each marker. Data represent the mean number of nuclei counted in more than 10 areas per plate for cultures from three embryos under each condition. t, time.

(D) GFP-positive cells, isolated as described in (A) through (C), were cultured in the presence or absence (Ctrl) of 0.5 μM 4-OHT. After 96 hr of culture, transcripts, as indicated, were analyzed by qPCR, shown relative to *Gapdh* transcripts, and standardized to the control as one. nd, not detectable.

(E–G) GFP-positive cells, isolated as for (A), were cultured in the presence or absence (Ctrl) of 0.5 μM 4-OHT added at the beginning of the culture (for 4-OHT) or after 72 hr (4-OHT^{72}) and processed for TUNEL staining at the times indicated. (E) TUNEL staining (green) of DAPI-treated cells after 96 hr of culture. White arrowheads point to TUNEL-positive cells. Scale bars, 20 μM. (F) Quantification of the percentage of TUNEL-positive cells at each time point. (G) After 96 hr of culture, qPCR of *p53* and *Noxa* transcripts.

In (C), (D), (F), and (G), n = 3 embryos; mean ± SD, *p < 0.05.

However, the phenotype of *Pitx2/3* mutant cells in culture appeared even more pronounced than in vivo, with the nearly complete absence of differentiated cells after 120 hr of culture. These differences suggested that culture conditions exacerbated the mutant phenotype. Since our standard primary culture conditions are under atmospheric (20%) oxygen, we postulated that oxidative stress might be implicated in cell survival failure of *Pitx2/3* mutant cells (Abbas et al., 2010). We thus investigated whether mutant cells exhibited higher levels of intracellular ROS than their controls at the onset of differentiation. To purify progenitor and differentiating muscle cells from embryos, we took advantage of the relative stability of the GFP reporter that continues to be detectable at a lower level in *Pax3*$^{GFP/+}$ differentiating cells, when *Pax3* is downregulated (Relaix et al., 2005;

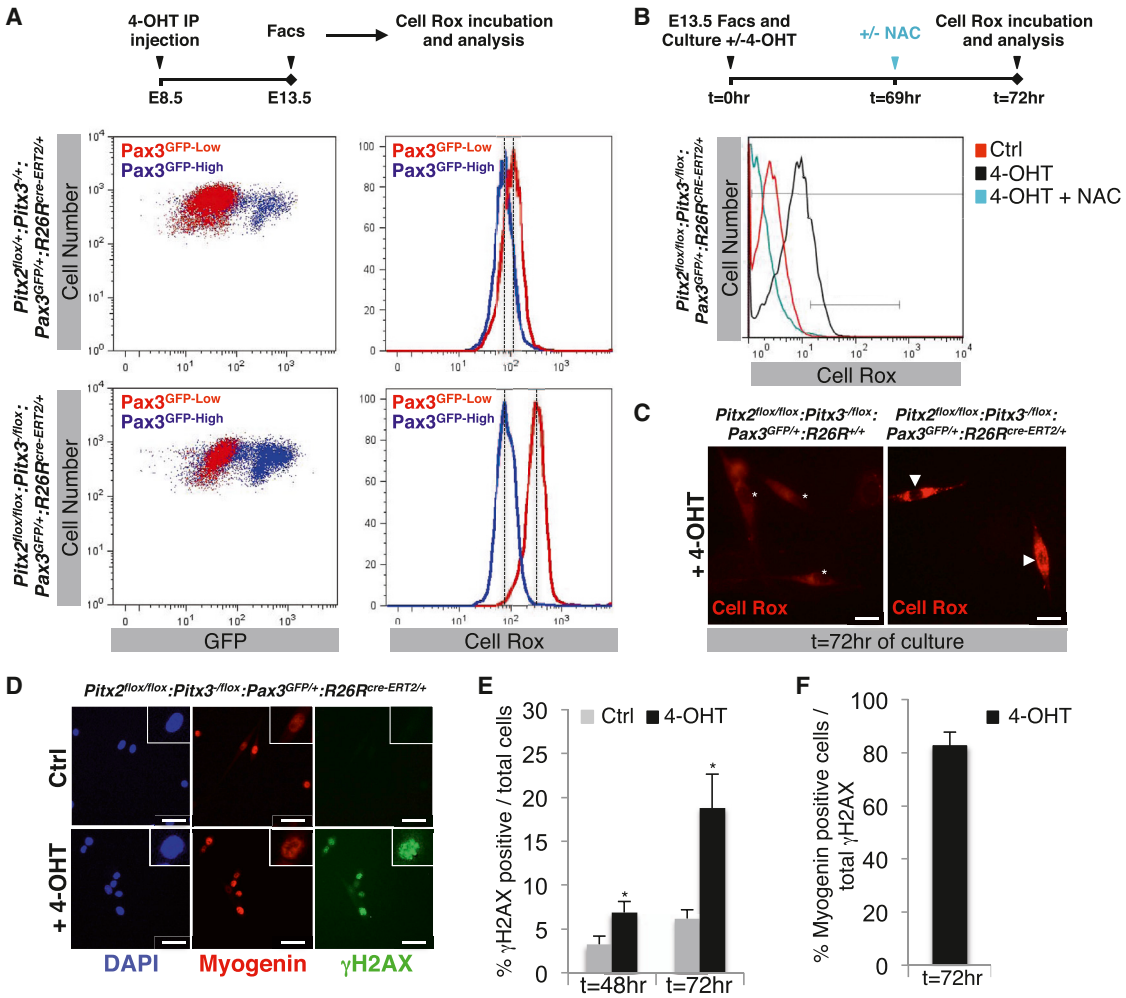

Figure 3. *Pitx2/3* Mutant Cells Accumulate Abnormal Levels of ROS, Leading to Apoptosis and Impaired Terminal Differentiation

(A) Mutant *Pitx2*$^{flox/flox}$:*Pitx3*$^{-/flox}$:*Pax3*$^{GFP/+}$:*R26R*$^{Cre-ERT2/+}$, and control *Pitx2*$^{flox/+}$:*Pitx3*$^{-/+}$:*Pax3*$^{GFP/+}$:*R26R*$^{Cre-ERT2/+}$ embryos at E13.5 were obtained by 4-OHT intraperitoneal injection of pregnant mothers at E8.5 and used for isolation by flow cytometry of two populations, Pax3$^{GFP-High}$ and Pax3$^{GFP-Low}$, based on their level of expression of GFP. Immediately after purification, cells were incubated with Cell Rox and analyzed by flow cytometry to measure GFP and Cell Rox fluorescence intensity.

(B) The whole GFP-positive cell population (High and Low), isolated from inducible mutant *Pitx2*$^{flox/flox}$:*Pitx3*$^{-/flox}$:*Pax3*$^{GFP/+}$:*R26R*$^{Cre-ERT2/+}$ embryos at E13.5, was cultured for 72 hr in the presence of 0.5 μM 4-OHT, incubated with Cell Rox, trypsinized, and analyzed by flow cytometry to measure fluorescence intensity. As a control, *Pitx2/3* mutant cells (+4-OHT) were treated with the antioxidant NAC (10 mM) for 3 hr before Cell Rox incubation.

(C) GFP-positive cells, isolated from control *Pitx2*$^{flox/flox}$:*Pitx3*$^{-/flox}$:*Pax3*$^{GFP/+}$:*R26R*$^{+/+}$ and inducible mutant *Pitx2*$^{flox/flox}$:*Pitx3*$^{-/flox}$:*Pax3*$^{GFP/+}$:*R26R*$^{Cre-ERT2/+}$ embryos at E13.5, were cultured for 72 hr in the presence of 0.5 μM 4-OHT, incubated with Cell Rox, and analyzed by fluorescence microscopy. Scale bars, 5 μM.

(D–F) In (D), GFP-positive cells, isolated as in (B), were cultured in the presence or absence (Ctrl) of 0.5 μM 4-OHT. After 48 hr and 72 hr of culture, cells were stained with DAPI and analyzed by immunocytochemistry using Myogenin and γH2AX antibodies. Scale bars in (D) represent 20 μM.

(E) γH2AX-positive cells were counted at 48 hr and 72 hr in control and mutant cultures, represented as the percentage of total cells.

(F) Myogenin-positive cells were counted and quantified as the percentage of total γH2AX-positive cells in the mutant (4-OHT) population at 72 hr (n = 3 embryos; mean ± SD, *p < 0.05).

Pallafacchina et al., 2010). Muscle cells from control and mutant embryos were separated by flow cytometry into Pax3$^{GFP-High}$ (Figure 3A, blue) and Pax3$^{GFP-Low}$ (Figure 3A, red) fractions and immediately processed for western blot analysis using Troponin T and phospho-histone-H3 antibodies (Figure S3E) or for ROS detection. Pax3$^{GFP-High}$ and Pax3$^{GFP-Low}$ populations of control and mutant cells were incubated with Cell Rox reagent, and the fluorescent signal was measured by flow cytometry (Figure 3A). First, using control cells, we noted a significant increase of ROS in Pax3$^{GFP-Low}$ differentiating cells, compared to Pax3$^{GFP-High}$ progenitor cells (Figure 3A). In mutant cells, this increase in Pax3$^{GFP-Low}$ cells was greatly enhanced, while, in contrast, progenitor cells (Pax3$^{GFP-High}$) had a similar level of ROS compared to controls. This abnormally high level of ROS in mutant differentiating cells was confirmed ex vivo by flow cytometry (Figure 3B) and by microscopy (Figure 3C) in control and mutant cells after 72 hr of culture. As expected, treatment of cells with N-acetyl-cysteine (NAC), a strong antioxidant that

scavenges intracellular ROS (Richards et al., 2011), completely reversed this upregulation (Figure 3B), demonstrating that deletion of *Pitx2/3* genes leads to an increase of oxidative stress in differentiating cells. Excessive ROS levels can lead to DNA damage (Karanjawala et al., 2002), which may trigger apoptosis if this reaches a critical threshold that compromises genomic stability (Shiloh, 2003). In *Pitx2/3* mutant cells, we found a significant increase of cells with γH2AX foci (Figures 3D and 3E), markers of DNA damage signaling (Bonner et al., 2008), compared to the control. It is important to note that this increase occurs at the onset of differentiation (t = 72 hr), in Myogenin-positive cells (Figures 3D and 3F) and correlates with the high level of intracellular ROS (Figures 3B and 3C). Overall, these results suggest that the excessive level of ROS observed in myogenic cells depleted of Pitx2/3 is responsible for the accumulation of irreversible DNA damage, leading to subsequent cell apoptosis.

To reduce the oxidative stress, we first performed cultures under 3% O_2. We observed a moderate reduction of apoptosis correlated with a small increase in differentiation in the absence of Pitx2/3 (Figures 4A and 4B); indeed, the low oxygen conditions had a minor effect on the level of intracellular ROS (Figure 4C). To efficiently decrease this level, we supplemented the culture medium with the antioxidant NAC at day 0 of culture and then followed the survival and differentiation of control and mutant cells after culture under 20% (Figures 4D–4H) and 3% O_2 (Figures 4F–4H). NAC treatment performed either under 20% or 3% O_2 culture conditions efficiently reduced the number of γH2AX-positive cells in *Pitx2/3* mutant cultures (Figure 4G), resulting in much less apoptosis of mutant cells (Figure 4H) and rescued differentiation (Figures 4B and 4C). Similar results were obtained using two different antioxidants, Trolox and Resveratrol (Figures S4A and S4B), thus demonstrating that the abnormal increase of ROS levels observed in cells depleted for Pitx2/3 is directly responsible for their altered terminal differentiation.

Pitx2/3 Fine-Tune the Expression of the Antioxidant System through Regulation of Nrf1 and Antioxidant Enzymes during Differentiation

ROS are formed as by-products of aerobic respiration and are mainly generated by the mitochondrial respiratory chain. Myogenic differentiation is accompanied by major metabolic changes, when cells switch from a glycolytic proliferative progenitor state to an oxidative postmitotic differentiated state (Remels et al., 2010; Blanchet et al., 2011). Such changes require extensive mitochondrial biogenesis that takes place at the onset of differentiation and leads to increased ROS production (Figure 3A; Malinska et al., 2012). To protect cells from oxidative damage, this intracellular oxidant activity needs to be balanced by an antioxidant system composed of scavenging and detoxifying enzymes (Sena and Chandel, 2012). It is interesting that *Aldh1a1*, encoding Aldehyde dehydrogenase 1a1, an enzyme that detoxifies oxidized aldehydic products (Vasiliou et al., 2004; Jean et al., 2011), had been identified previously as a direct target of Pitx3 in midbrain dopaminergic neurons (Jacobs et al., 2007). We therefore investigated whether Pitx2/3 may regulate part of the antioxidant system in muscle cells leading to increased ROS levels in their absence. We first assessed in vivo expression of the antioxidant system. $Pax3^{GFP\text{-}High}$ and $Pax3^{GFP\text{-}Low}$ fractions were isolated from control E13.5 $Pax3^{GFP/+}$ embryos and processed for mRNA extraction. Transcript levels for markers of mitochondrial function (Cox5a, NdUfv1; Bourens et al., 2013) and oxidative metabolism (PGC1α, Eno3; Patti et al., 2003) demonstrated the metabolic shift occurring at the onset of differentiation in $Pax3^{GFP\text{-}Low}$ cells (Figures 5A and S5A). We found significant upregulation of antioxidant genes in these cells compared to $Pax3^{GFP\text{-}High}$ progenitor cells (Figures 5A and S5A), thus establishing a direct correlation between the metabolic shift occurring at the onset of differentiation and the activation of the antioxidant system. We then examined the kinetics of this coregulation ex vivo. Consistent with the in vivo results, most of the antioxidant genes were found to be upregulated at 72 hr of culture, when the major onset of differentiation occurs and the expression of both *Pitx2/3* genes increases (Figure S5B). We next investigated whether this activation occurs normally during differentiation of *Pitx2/3* mutant cells. Quantification of mRNA levels after 72 hr of culture revealed an upregulation of transcripts for Gpx3 and PGC1α in mutant cells (Figure 5B), an expected response to the abnormal increase of ROS (Ufer and Wang, 2011). We also observed a concomitant and consistent decreased expression of Aldh1a1, Mt1, Gsta1, Nrf1, and SOD1 in mutant cells compared to controls both at mRNA (Figure 5B) and at protein levels (Figure 5D). This decrease was confirmed in vivo in $Pax3^{GFP\text{-}Low}$ cells isolated from control and mutant embryos (Figure 5C) and, as expected, leads to a significant reduction of the total antioxidant capacity (TAC) of differentiating *Pitx2/3* mutant cells both in vivo and ex vivo (Figures 5E and S5C).

We next investigated the molecular mechanism underlying the decreased expression of this antioxidant system in Pitx2/3-depleted cells. In silico analysis shows that the promoters of antioxidant genes such as *SOD1, Mt1*, *Gsta1*, and *Aldha1a* also have binding sites for the nuclear respiratory factor 1 (Nrf1) (Satoh et al., 2013), now commonly abbreviated as NRF1 but referred to here as Nrf1. In view of the downregulation of Nrf1 in *Pitx2/3* mutant cells (Figure 5B), we postulated that Pitx2/3 might regulate antioxidant genes through the direct activation of *Nrf1*. Using ChIP on E13.5 embryos, we first showed a strong recruitment of Pitx2/3 on *Pitx response elements* (*PitxRE*) local-ized in regulatory regions of *Nrf1* (Figure 5F). Pitx2 and Pitx3 can transactivate these regions in a heterologous cell system, and mutations of both *PitxRE* completely abolish this activation (Figure 5G). We found a similar activation of the *Aldh1a1* promoter by Pitx2 and Pitx3, consistent with strong recruitment of both Pitx2/3 on these sequences in vivo (Figure 5H). We also observed direct binding of Nrf1 to *Mt1*, *SOD1*, and *Gsta1* regulatory regions in vivo (Figure 5H). Analysis of the *Aldh1a1* promoter revealed the presence of a nuclear respiratory factor binding site, and efficient binding of Nrf1 to this sequence was confirmed (Figure 5H), suggesting a possible coregulation of antioxidant genes by both Pitx2/3 and Nrf1. To investigate this hypothesis, we searched in silico for *PitxRE* near *nuclear respiratory factor binding sites* and identified the presence of both sites in the regulatory environment of *Mt1*, *SOD1*, and *Gsta1* genes, in agreement with our ChIP identification of Pitx2/3 on these regulatory regions (Figure 5H). Taken together with our analysis of ROS levels in control and mutant cells (Figures 3A–3C), these results thus support a two-level regulation of the antioxidant pathway by Pitx2/3 (Figure 5I), occurring at the onset of differentiation when high metabolic needs require extensive

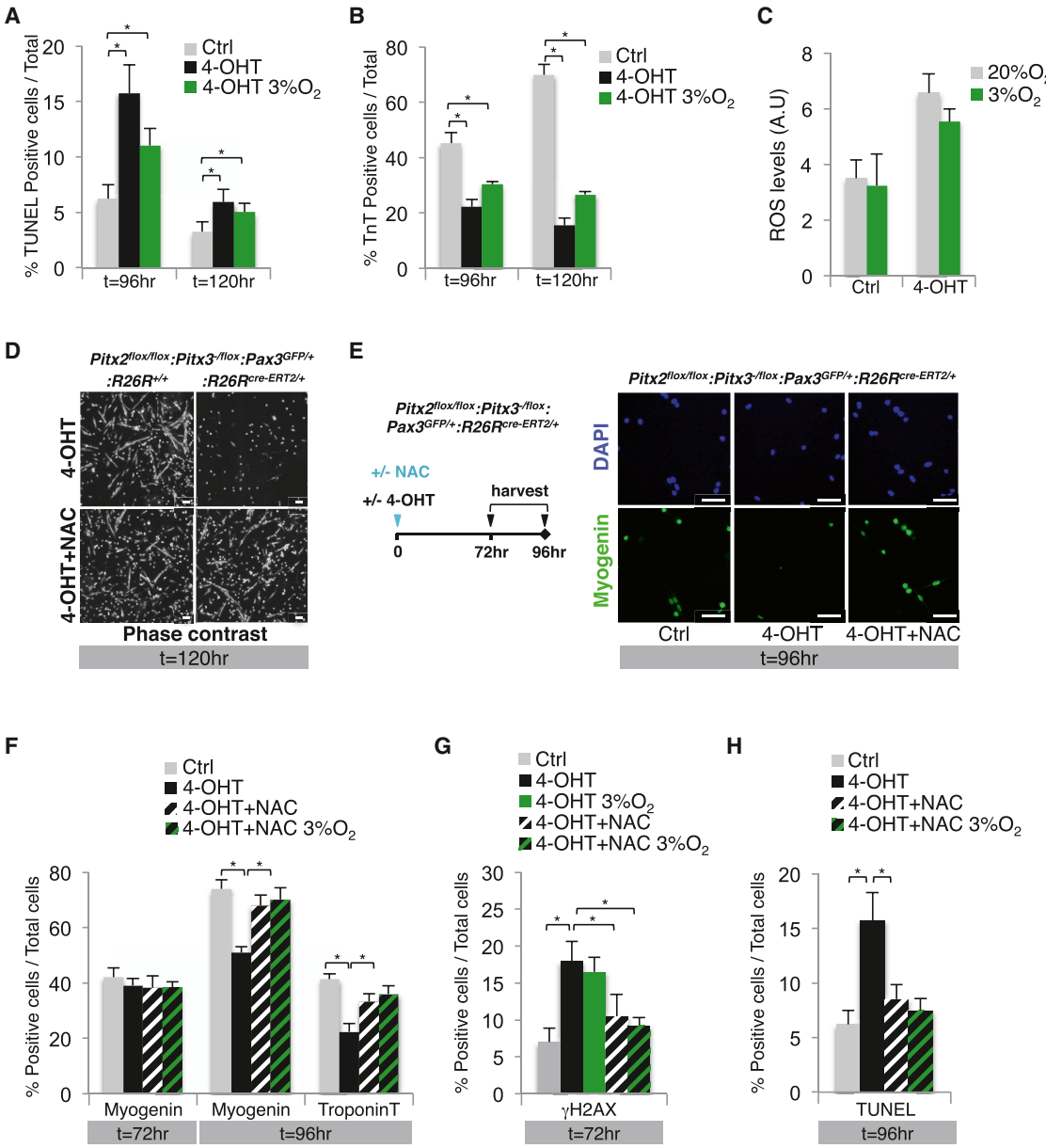

Figure 4. Rescue of the Differentiation Defect of *Pitx2/3* Mutant Cells by Use of Antioxidants

(A–C) GFP-positive cells, isolated from inducible mutant *Pitx2*$^{flox/flox}$:*Pitx3*$^{-/flox}$:*Pax3*$^{GFP/+}$:*R26R*$^{Cre-ERT2/+}$ embryos at E13.5, were cultured in the presence (4-OHT) or absence (Ctrl) of 0.5 μM 4-OHT. Cells were either cultured under 20% O_2 (Ctrl and 4-OHT) or 3% O_2 (4-OHT 3% O_2) for 96 hr and 120 hr and processed for (A) TUNEL staining and (B) Troponin T (TnT) staining or (C) incubated with Cell Rox, trypsinized, and analyzed by flow cytometry to measure fluorescence intensity. (A) TUNEL-positive cells or (B) Troponin T-positive cells were counted and quantified as the percentage of total cells. ROS levels are expressed as absolute units (A.U.) (n = 3 embryos; mean ± SD, *p < 0.05).

(D–H) GFP-positive cells, isolated from inducible mutant *Pitx2*$^{flox/flox}$:*Pitx3*$^{-/flox}$:*Pax3*$^{GFP/+}$:*R26R*$^{Cre-ERT2/+}$ embryos at E13.5, were cultured in the presence of 0.5 μM 4-OHT with or without 5 mM NAC (added at t^0). Cells were cultured either under 20% O_2 (Ctrl and 4-OHT) or 3% O_2 (4-OHT, 3% O_2; 4-OHT + NAC, 3% O_2). Cells were visualized under phase contrast after 120 hr of culture, as shown in (D), or analyzed by immunocytochemistry with Myogenin, Troponin T, and γH2AX antibodies and by the TUNEL reaction after 72 hr or 96 hr of culture, as shown in (E) through (H). In (E), immunofluorescence on DAPI-stained cells with a Myogenin antibody after 96 hr of culture is shown. In (F) through (H), Myogenin-, Troponin T-, γH2AX-, and TUNEL-positive cells were counted and quantified as the percentage of total cells (n = 4 embryos; mean ± SD, *p < 0.05). Scale bars, 20 μM.

mitochondrial biogenesis. To investigate whether such regulation can also occur in the absence of metabolic demand, control and mutant cells were treated when still proliferating, after 36 hr of culture, with buthionine sulfoximine (BSO), an inhibitor of γ-glutamylcysteine synthetase (Griffith 1982) to deplete glutathione (GSH). In contrast to control cells in which such depletion (Figure S5E) leads to significant induction of the antioxidant pathway (Figure S5F), and thus moderate increase of ROS levels

and apoptosis (Figures S5G and S5H), analysis of *Pitx2/3* mutant cells revealed a defective activation of this pathway leading to a large increase of ROS levels and cell death after 18 hr of treatment (Figures S5G and S5H). These results demonstrate the essential role of Pitx2 and Pitx3 in the activation of antioxidant genes in response to high levels of ROS induced either by increase of metabolic activity during differentiation or acute induced oxidative stress.

Pitx2/3 Mutant Cells Exhibit Defective Mitochondrial Function, Leading to Overproduction of ROS during Differentiation

To investigate whether the defective activation of the antioxidant pathway is sufficient to induce the abnormally high levels of intracellular ROS observed in *Pitx2/3* mutant cells, wild-type fetal cells isolated from *Pax3*$^{GFP/+}$ embryos were transfected with siRNA directed against *SOD1*, *Mt1*, and *Gsta1* transcripts (Figure 6A). Efficient inhibition of the expression of these three genes (Figure S6A) leads to severe apoptosis of cells after 96 hr of culture (Figure 6C), as a consequence of an increase of ROS levels (Figure 6B); however, while significant, this increase does not reach that of *Pitx2/3* mutant cells. This result suggested that the defective expression of scavenging enzymes was not sufficient to induce the high ROS levels of Pitx2/3-deficient cells. In addition to its regulation of antioxidant genes, Nrf1 also plays a key role in integrating the transcription of nuclear- and mitochondrial-encoded genes. Nrf1 target genes include subunits of the mitochondrial respiratory complexes such as *cytochrome C*, and the transcription factor A *Tfam*, which transcribes the mitochondrial genome (Kelly and Scarpulla, 2004). As alteration in expression of these genes can lead to mitochondrial dysfunction, a major cause of ROS overproduction, we investigated their expression in *Pitx2/3* mutant cells. Quantification of their transcripts both in vivo in Pax3$^{GFP\text{-}Low}$ cells isolated from control and mutant embryos (Figure 6D) and ex vivo after 72 hr of culture (Figure S6B) revealed a consistent decrease of their expression as well as that of two Tfam target genes *Ndufv1* and *Ndufb6*. We then investigated markers of mitochondrial function in mutant cells compared to controls and observed an alteration of the cellular bioenergetic state as evidenced by the decrease in the NAD+/NADH ratio (Figures 6E and S6C), together with a reduction in the intracellular ATP content (Figure 6F). Quantification of mitochondrial ROS by incubation of cells with Mitosox after 72 hr of culture revealed a higher rate of ROS production in mutant cells compared to controls (Figure 6G). Overall, these results suggest that, in *Pitx2/3* mutant cells, the altered expression of Nrf1 and of its target genes is responsible for both mitochondrial dysfunction, leading to ROS overgeneration, and concomitant defective expression of the antioxidant system, leading to decreased ROS scavenging. As these two events occur at the onset of differentiation, when high metabolic needs require increased oxidative phosphorylation, we investigated whether inhibition of mitochondrial biogenesis, and thus of oxidative phosphorylation, by depletion of Tfam (Lee et al., 2011) might prevent mutant cell differentiation and their apoptosis. *Pitx2/3* mutant cells were transfected with siRNA directed against *Tfam* (Figure 6H). As expected, the inhibition of *Tfam* expression (Figure S6D) prevented mutant cell differentiation (Figure 6I), leading to an increase in cell number by maintenance of proliferation and to a significant rescue of apoptosis (Figure 6J).

To confirm the direct correlation between Nrf1 downregulation and the phenotype of Pitx2/3-deficient cells, we restored Nrf1 expression in mutant cells through lentiviral infection. As expected, Nrf1 overexpression (Figure S7A) prevented the abnormal increase of ROS (Figure 7C) both by activating the expression of the antioxidant system and by preventing mitochondrial dysfunction through rescued expression of Tfam (Figure S7B). This resulted in a significant rescue of the differentiation of mutant cells, as evidenced by Troponin T expression (Figures 7A and 7B) and the level of *Myogenin* transcripts (Figure S7A). We therefore conclude that Pitx2/3, through their control of the *Nrf1* gene, are critical regulators of the redox state of myogenic cells and that this is necessary for their survival and their differentiation.

DISCUSSION

Our analysis of the role of Pitx2 and Pitx3 during fetal myogenesis reveals an essential role in regulation of intracellular redox levels during differentiation (Figure 7D). In their absence, ROS accumulate to pathological levels at the onset of differentiation, leading to DNA damage and consequent death of differentiating cells (Figure 7E).

Major metabolic changes occur as cells become more specialized within a differentiated lineage. In the case of myogenic cells, these changes are of particular interest, specifically as cells switch from a glycolytic proliferative progenitor state to an oxidative postmitotic differentiated state. Previous studies have correlated this metabolic shift with an increase of intracellular ROS levels in immortalized adult cell lines (Malinska et al., 2012; Lee et al., 2011). However, very little is known about redox levels of myogenic cells in vivo during development or about the regulation of genes involved in ROS control (Sena and Chandel, 2012). We have found an increase of ROS levels occurring in vivo at the onset of differentiation and have identified the Pitx2/3 transcription factors as essential regulators of this process. In *Pitx2/3* mutant muscle cells, ROS increase is deregulated, leading to excessive accumulation of ROS and further cell death. We have shown that this is due to downregulation of the nuclear respiratory factor 1 (Nrf1), a transcription factor that is essential for the coordination of mitochondrial function (Kelly and Scarpulla, 2004) and that we identified as critical for the fine-tuning of the level of antioxidant enzymes. The decreased expression of Nrf1 and a subset of its targets are responsible for both impaired mitochondrial activity leading to ROS overgeneration and deficient activation of the antioxidant pathway (Figures 7C and 7D). Furthermore, using ChIP, transactivation assays, and lentiviral rescue, we show direct regulation of *Nrf1* by Pitx2/3 with joint binding of Nrf1 and Pitx2/3 on downstream antioxidant target genes. These results place Pitx2/3 as core regulators of redox control during myogenic differentiation.

It is interesting that expression of the detoxifying enzyme, Aldh1a1, is downregulated in *Pitx2/3* mutant muscle and that direct regulation by Pitx3 was also shown in midbrain dopaminergic neurons (Jacobs et al., 2007). In these neurons, Pitx3 has a survival function (van den Munckhof et al., 2003), and Parkinson's disease, in which Pitx3-positive dopaminergic neurons are specifically affected, has been linked to oxidative stress

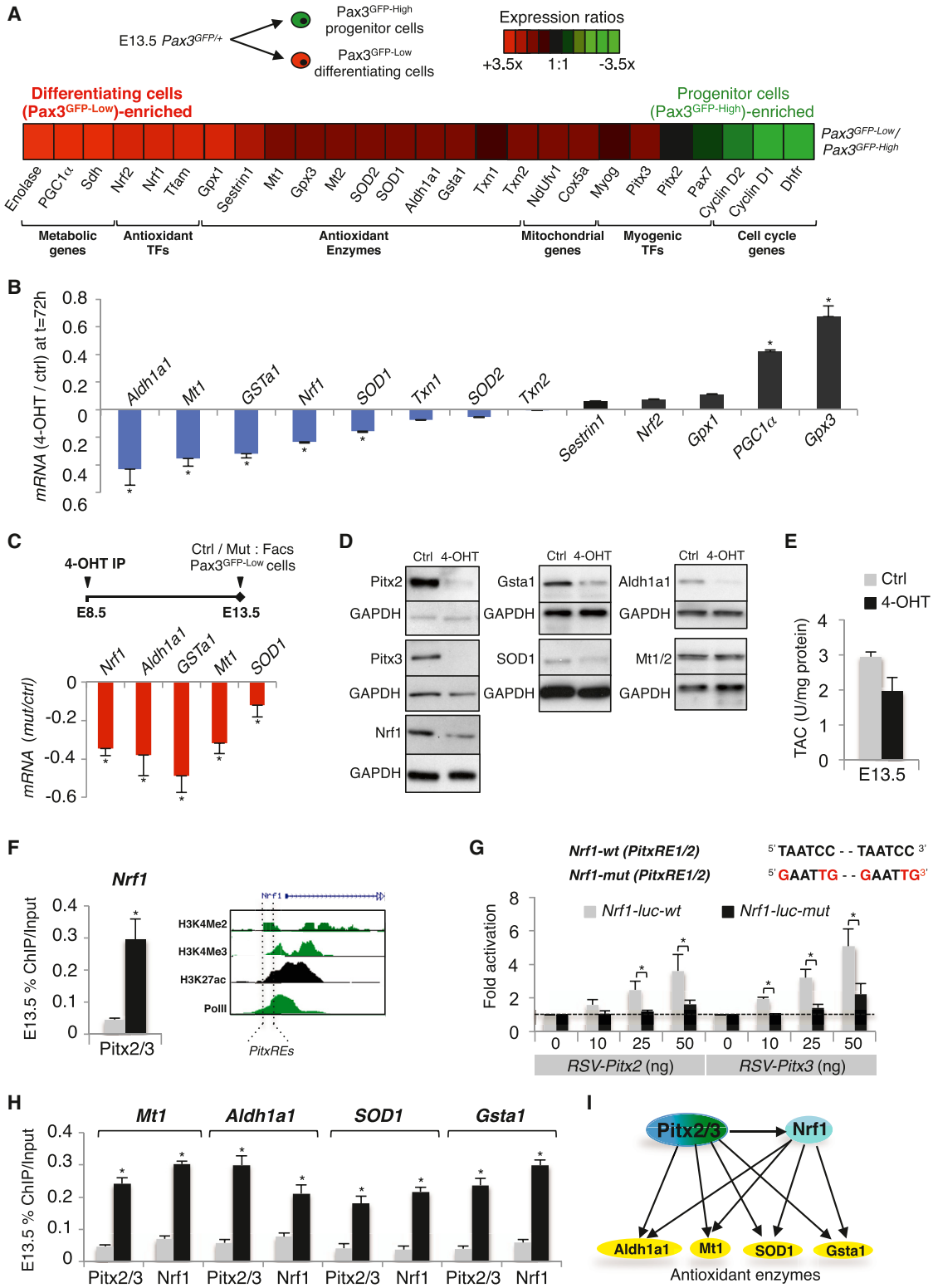

Figure 5. Pitx2/3 Directly Regulate Transcription Factors and Enzymes that Protect against Oxidative Damage

(A) Two populations, Pax3$^{GFP-High}$ and Pax3$^{GFP-Low}$, were isolated by flow cytometry from *Pax3$^{GFP/+}$* embryos at E13.5 based on their level of expression of GFP. RNA samples were analyzed by qPCR for transcripts of proliferation markers, myogenic transcription factors, antioxidant enzymes and transcription factors, and mitochondrial and metabolic genes, relative to the level of *Gapdh* transcripts. The data are represented as a heat map.

(legend continued on next page)

(Varçin et al., 2011). Similarly in the eye, in both the retina where Pitx2 is expressed and in the Pitx3-positive lens, mutations in mice and humans have been associated with downregulation of *Aldh1a1* (Paylakhi et al., 2011) and with glaucoma and cataracts (Amendt et al., 1998; Semina et al., 1996, 1997), two disorders in which oxidative stress has also been implicated (Babizhayev, 2012). We therefore speculate that the regulation of the redox state that we have identified during fetal myogenesis is a common property of Pitx transcription factors at their different sites of expression.

In vivo, the cell death that we observed in developing fetal muscle masses in the absence of Pitx2/3 leads to a striking deficit in skeletal muscle. This is observed when the conditional *Pitx2/3* alleles are mutated early in paraxial mesoderm, using the *MSD-Cre* line, but not when the deletion occurs in differentiated muscle fibers, using the *HSA-Cre* line. This is consistent with a role of Pitx2/3 in activation of the antioxidant pathways through Nrf1 and its target genes and with their role at the onset of differentiation. Embryonic and fetal myoblasts have characteristic properties (Biressi et al., 2007), and distinct transcriptional regulators of embryonic and fetal muscle differentiation have begun to be identified (Hutcheson et al., 2009; Messina et al., 2010). Expression of the myogenic determination gene *MyoD* is not compromised in the *Pitx2/3* mutant at fetal stages, a phenotype that differs from that in embryonic muscle, where Pitx2, acting downstream of Pax3, is required for *MyoD* expression through direct activation of the *MyoD* embryonic enhancer (L'honoré et al., 2010). These different functional requirements for Pitx factors underline the differences between embryonic and fetal myogenesis. In the context of oxidative stress, with the introduction of the chorio-allantoic circulation, the fetus is exposed to higher oxygen levels (Ufer and Wang, 2011), making it more vulnerable to the increase of ROS observed in the absence of Pitx2/3 than during embryonic myogenesis when it is less deleterious.

During fetal myogenesis, we show that ROS levels become abnormally high at the onset of differentiation in the absence of Pitx2/3, leading to accumulation of DNA lesions marked by γH2AX foci in Myogenin-positive cells. DNA lesions due to oxidation are processed by the base excision repair pathway (Narciso et al., 2007). In myogenic cells, this pathway is activated in proliferating cells before differentiation and involves cell cycle arrest coupled with a transient block of transcription of muscle-specific genes referred to a differentiation checkpoint (Puri et al., 2002). Such a mechanism, which would permit genome repair before the differentiation program begins, is no longer present in differentiating cells (Narciso et al., 2007). We provide evidence that myogenic cells at the onset of differentiation, which cannot activate the base excision repair pathway, rely upon apoptosis as a cellular response to oxidative DNA damage.

In conclusion, the myogenic system clearly illustrates the importance of regulating the redox state at the onset of cell differentiation. During fetal myogenesis, Pitx2/3 control this redox state through the regulation of Nrf1 and of antioxidant pathways. Their absence results in a major upregulation of ROS levels which reach a pathological threshold with consequent death of differentiating cells. The Pitx2/3 transcription factors are thus key regulators of the intracellular redox state during development.

EXPERIMENTAL PROCEDURES

Animal Handling and Genotyping

Pitx2-floxed (*Pitx2*$^{flox/+}$) mice were generously provided by S. Camper and P. Gage. *Pitx3-floxed(neo)* (*Pitx3*^{flox}) and *Pitx3* null (Pitx3^{-}) alleles have been already described elsewhere (L'Honoré et al., 2007). The *Pitx3*^{flox} allele with *neo* is a hypomorph, expressed as 50% of the wild-type allele. As *Pitx2*$^{-/flox}$:*Pitx3*$^{-/flox}$ mice are barely viable and fertile, we used *Pitx2*$^{flox/flox}$:*Pitx3*$^{-/flox}$ mice. *Pax3*$^{Cre/+}$, *HSA-Cre*, and *MSD-cre* mice were generously given by J. Epstein (Engleka et al., 2005), J. Melki (Miniou et al., 1999), and A. Gossler (Beckers et al., 2000), respectively. *R26R*$^{mTomato-STOP-mGFP/+}$, *R26R*$^{CRE-ERT2/+}$, and *R26R*$^{flox-lacZ/+}$ reporter mice were obtained from the Jackson Laboratories. Genotyping was carried out by PCR using DNA isolated from the amniotic membrane of embryos or from adult tail sections. All animal procedures were approved and conducted in accordance with the Institut Pasteur animal ethics committee, following the regulations of the Ministry of Agriculture and the European Community guidelines.

(B) GFP-positive cells isolated from conditional mutant *Pitx2*$^{flox/flox}$:*Pitx3*$^{-/flox}$:*Pax3*$^{GFP/+}$:*R26R*$^{Cre-ERT2/+}$ embryos were cultured in the presence (4-OHT) or absence (Ctrl) of 0.5 μM 4-OHT. After 72 hr of culture, samples were analyzed by qPCR for transcripts of antioxidant transcription factors and enzymes relative to *Gapdh* transcripts in mutant/control cells, expressed as a log ratio (n = 3 embryos; mean ± SD, *p < 0.05).

(C and D) Mutant *Pitx2*$^{flox/flox}$:*Pitx3*$^{-/flox}$:*Pax3*$^{GFP/+}$:*R26R*$^{Cre-ERT2/+}$ and control *Pitx2*$^{flox/+}$:*Pitx3*$^{-/+}$:*Pax3*$^{GFP/+}$:*R26R*$^{Cre-ERT2/+}$ embryos at E13.5 were obtained by 4-OHT intraperitoneal injection of pregnant mothers at E8.5 and used for isolation by flow cytometry of the Pax3$^{GFP-Low}$ population.

(C) RNA was analyzed by qPCR for antioxidant enzyme transcripts relative to *Gapdh* transcripts in control/mutant (Ctrl/Mut) cells, expressed as a log ratio (n = 2 embryos; mean ± SD, *p < 0.05).

(D) GFP-positive cells isolated from *Pitx2*$^{flox/flox}$:*Pitx3*$^{-/flox}$:*Pax3*$^{GFP/+}$:*R26R*$^{CRE-ERT2/+}$ embryos were cultured for 72 hr in the presence (+4-OHT) or absence (Ctrl) of 0.5 μM 4-OHT and processed for protein extraction. Western blot analysis indicated the level of Pitx2, Pitx3, Nrf1, SOD1, Mt1, Gsta1, and Aldh1a1 proteins.

The experiments were performed with three independent cultures, and a representative experiment is shown.

(E) Antioxidant total capacity was measured (n = 3 embryos; mean ± SD, *p < 0.05).

(F) ChIP analysis for the presence of Pitx2/3 on *Nrf1* regulatory sequences (black) and negative control regions (gray), as indicated, was performed on chromatin isolated from the trunk and limbs of wild-type embryos at E13.5. The location of *PitxREs*, histone marks for active chromatin and RNA polymerase II (Pol II) binding, is indicated for the *Nrf1* gene on the right.

(G) Activation of the *Nrf1* promoter by Pitx2 and Pitx3. 293 cells were transfected with a luciferase reporter construct containing Nrf1 regulatory sequences (*Nrf1-wt-luc*). Dose response is shown for cotransfection of increasing amounts of Pitx2 and Pitx3 expression plasmids. Mutations of both PitxRE prevented transactivation (n = 3 independent experiments, each performed in duplicate, mean ± SD, *p < 0.05).

(H) ChIP analysis for the presence of Pitx2/3 and Nrf1 on *Mt1*, *Aldh1a1*, *SOD1*, and *Gsta1* regulatory sequences was carried out on chromatin prepared from the trunk and limbs of wild-type embryos at E13.5. The y axis shows the average percentage of immunoprecipitation compared to input for regulatory regions of each gene (black) or negative control regions (gray) located close to each gene. Results presented are the average ± SD of three different ChIP experiments performed on three independent chromatin preparations, *p < 0.05.

(I) Scheme for proposed targets of Pitx2/3 and Nrf1.

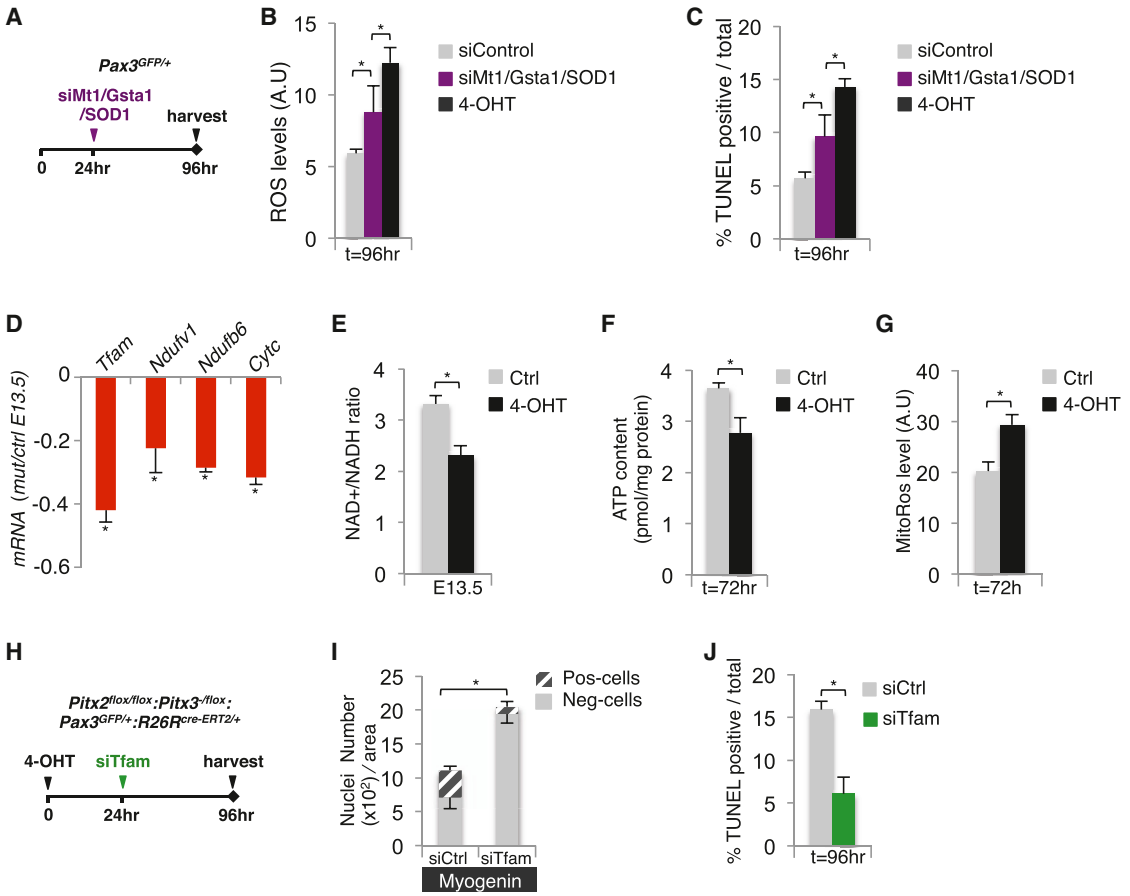

Figure 6. *Pitx2/3* Mutant Cells Are Characterized by Impaired Mitochondrial Function at the Onset of Differentiation

(A–C) GFP-positive cells from *Pax3*$^{GFP/+}$ embryos at E13.5 were separated by flow cytometry and cultured. (A) Cells were transfected 24 hr after plating with siRNA directed against *SOD1, Gst1a*, and *Mt1* transcripts or with siControl. As a positive control, GFP-positive cells from inducible mutant *Pitx2*$^{flox/flox}$*:Pitx3*$^{-/flox}$*:Pax3*$^{GFP/+}$*:R26R*$^{CRE-ERT2/+}$ embryos at E13.5 were separated by flow cytometry and cultured in the presence of 4-OHT without any transfection. After 96 hr of culture, cells were (B) processed for quantification of ROS content with Cell Rox, expressed as absolute units (A.U.), or (C) analyzed by immunocytochemistry using the TUNEL reaction. TUNEL-positive cells were counted and quantified as the percentage of total cells (n = 3 independent transfections, each performed in duplicate; mean ± SD, *p < 0.05).

(D and E) Mutant *Pitx2*$^{flox/flox}$*:Pitx3*$^{-/flox}$*:Pax3*$^{GFP/+}$*:R26R*$^{CRE-ERT2/+}$ and control *Pitx2*$^{flox/+}$*:Pitx3*$^{-/+}$*:Pax3*$^{GFP/+}$*:R26R*$^{CRE-ERT2/+}$ embryos at E13.5 were obtained by 4-OHT intraperitoneal injection of pregnant mothers at E8.5 and used for isolation by flow cytometry of the Pax3$^{GFP-Low}$ population.

(D) RNA was analyzed by qPCR for transcripts of *Tfam* and respiratory chain components relative to *Gapdh* transcripts in mutant (mut) /control (ctrl) cells, expressed as a log ratio (n = 2 embryos; mean ± SD, *p < 0.05).

(E) Pax3$^{GFP-Low}$ cells were used after purification for quantification of the NAD+/NADH ratio (n = 2 embryos; mean ± SD, *p < 0.05).

(F and G) GFP-positive cells isolated from conditional mutant *Pitx2*$^{flox/flox}$*:Pitx3*$^{-/flox}$*:Pax3*$^{GFP/+}$*:R26R*$^{CRE-ERT2/+}$ embryos were cultured in the presence (4-OHT) or absence (Ctrl) of 0.5 μM 4-OHT. After 72 hr of culture, samples were processed for (F) quantification of ATP content and (G) mitochondrial ROS levels expressed as absolute units (A.U.) (n = 3 embryos for each gene; mean ± SD, *p < 0.05).

(H–J) GFP-positive cells isolated from conditional mutant *Pitx2*$^{flox/flox}$*:Pitx3*$^{-/flox}$*:Pax3*$^{GFP/+}$*:R26R*$^{CRE-ERT2/+}$ embryos were cultured in the presence of 0.5 μM 4-OHT. After 24 hr of culture, cells were transfected with siRNA directed against *Tfam* transcripts or siControl. Cells were processed for immunohistochemistry using (I) Myogenin antibodies or (J) TUNEL staining at 96 hr. (I) Results were quantified by counting positive and negative nuclei. Data represent the mean number of nuclei counted in more than 10 areas per plate for cultures from three independent transfections. (J) TUNEL-positive cells were counted and quantified as the percentage of total cells (n = 3 embryos; mean ± SD, *p < 0.05).

Whole-Mount In Situ Hybridization and X-Gal Staining

Mouse embryos were collected after natural overnight mating. Noon of the day on which a vaginal plug was detected was considered as E0.5, and embryos were staged by counting the number of somites. Whole-mount in situ hybridization was performed as previously described (L'honoré et al., 2010), using digoxigenin-labeled riboprobes for *Myogenin*. Whole-mount X-Gal and whole-mount antibody staining were performed as described elsewhere (Coulon et al., 2007; Grégoire and Kmita, 2008) with modifications (see Supplemental Information).

Immunohistochemistry, Immunofluorescence, and Western Blot

Western blot, immunohistochemistry, and immunofluorescence were carried out as described elsewhere (L'Honoré et al., 2007; Relaix et al., 2006). Antibodies and kits used for TUNEL assay and EdU staining are detailed in the Supplemental Information. GFP and Tomato detection and pictures were obtained using an Apotome.

Primary Cell Purification and Culture

E13.5 embryos were dissected to obtain trunk and limbs. Care was taken to eliminate internal organs and the neural tube. Embryo tail fragments were

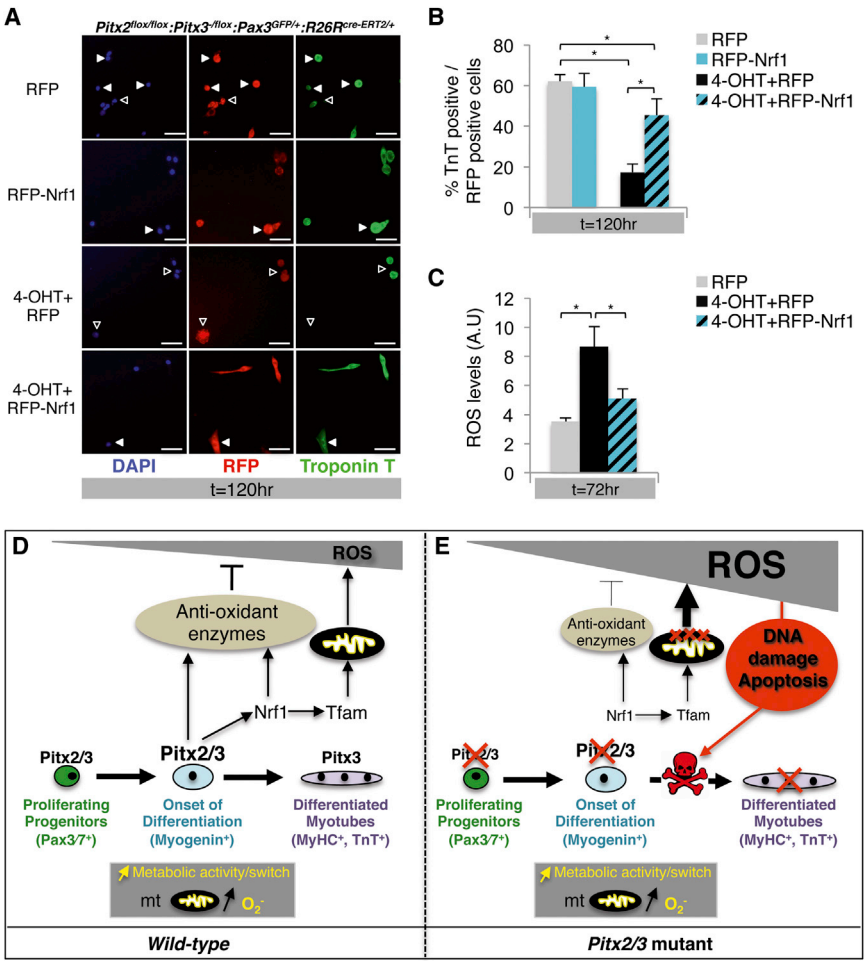

Figure 7. Rescue of the Differentiation Defect of *Pitx2/3* Mutant Cells by Nrf1 Expression

(A–C) GFP-positive cells from inducible mutant *Pitx2*$^{flox/flox}$:*Pitx3*$^{-/flox}$:*Pax3*$^{GFP/+}$:*R26R*$^{CRE-ERT2/+}$ embryos at E13.5 were separated by flow cytometry and cultured in the presence (4-OHT) or absence (Ctrl) of 0.5 μM 4-OHT. Fourteen hours after plating, cells were infected with lentiviral particles expressing the red fluorescent protein (RFP) reporter gene alone or Nrf1 with the reporter RFP (RFP-Nrf1).

(A) After 120 hr of culture, control and mutant cells were stained with DAPI and analyzed by immunocytochemistry using RFP (red) and Troponin T (green) antibodies.

(B) RFP- and Troponin T-double-positive cells were counted and quantified as a percentage of total RFP-positive cells (n = 5 embryos; mean ± SD, *p < 0.05).

(C) After 72 hr of culture, cells transduced by RFP or RFP-Nrf1 were incubated with Cell Rox, trypsinized, and analyzed by flow cytometry to measure fluorescence intensity. (n = 3 embryos for each gene; mean ± SD, *p < 0.05).

(D and E) In (D), a model of *Pitx2/3* gene function during fetal myogenesis is shown: *Pitx2/3* genes prevent excessive oxidative stress during differentiation through the regulation of *Nrf1* and genes for antioxidant enzymes. (E) In their absence, differentiating cells accumulate excessive ROS levels due to low expression of antioxidant enzymes and defective mitochondrial respiration, leading to DNA damage and apoptosis. MyHC, myosin heavy chain; TnT, troponin; Mt, mitochondria.

conserved for genotyping. Cells were then prepared and cultured as described elsewhere (Montarras et al., 2005; Relaix et al., 2006) with modifications (see Supplemental Information). 4-OHT was prepared and used as described elsewhere (Lepper et al., 2009) with modifications (see Supplemental Information). NAC (Sigma) was diluted at 0.5 M in H_2O before each experiment and used for cell seeding at 5 mM in growth medium or added to cell culture at 10 mM 3 hr before Cell Rox analysis. Resveratrol (Enzo Life Sciences) was diluted at 0.05 M in EtOH before each experiment and added to cell culture at 25 μM. Trolox (Abcam) was stored as a 1 mM solution at −20°C in DMSO and added at 10 μM to cell cultures. BSO (Enzo Life Sciences) was diluted at 5 mM in H_2O before each experiment and added to cell cultures at 10 μM.

RNA Extraction and Quantitative Real-Time PCR Analysis

Cells were collected after flow cytometry in RLT buffer (QIAGEN) for RNA extraction or plated on gelatin-coated dishes in growth medium supplemented, or not supplemented, with 4-OHT and/or NAC before RNA extraction. Total RNA was extracted and purified after DNase treatment (Promega) using the RNAeasy Micro kit (QIAGEN) and was reverse-transcribed into cDNA, based on instructions provided by the Transcriptor cDNA synthesis kit (Roche). Quantitative real-time PCR was performed on a StepOnePlus PCR machine (Applied Biosystems) using the FastStart Universal SYBR Green Master (Roche).

Metabolic Analysis

ROS quantification was performed by microscopy or flow cytometry using the Cell ROX and the MitoSOX probes (Invitrogen). The following kits were used for metabolic analysis according to manufacturer's instructions: TAC kit (Abcam), GSH colorimetric detection kit, and NAD+/NADH detection and ATP quantification kits (BioVision). For details about these methodologies, see Supplemental Information.

ChIP

ChIP was performed as described elsewhere (Coulon et al., 2007; Navarro et al., 2010) with modifications (see Supplemental Information).

Lentiviral Production, Cell Infection, siRNA Transfection, and Transactivation Assays

Lentiviral vectors CMV-NRF1-RFP-2A and RFP-2A were purchased from abm. siRNA were purchased from Origene (Tfam) and Santa Cruz Biotechnology (Mt1, Gsta1, SOD1). *Tfam* and *Aldh1a1* promoter mutants were generated using a commercial kit (Stratagene) according to the manufacturer's instructions and transfected into 293 cells. Details about these methodologies can be found in the Supplemental Information.

Statistical Analysis

All experiments were carried out on a minimum of three embryos. All data are presented as mean and SD. The Student's t test was applied. A p value < 0.05 was considered statistically significant.

SUPPLEMENTAL INFORMATION

Supplemental Information includes Supplemental Experimental Procedures and seven figures and can be found with this article online at http://dx.doi.org/10.1016/j.devcel.2014.04.006.

ACKNOWLEDGMENTS

This work was supported by the Institut Pasteur and the CNRS (URA 2578), with grants to M.B. and D.M. from the Association Française contre les Myopathies, the Agence Nationale pour la Recherche (REGSAT), and the E.U. OptiStem project (Health, FP7-2007, 223098) and to J.D. from the Canadian Institute of Health Research (MT-15081). A.L.H., M.B., and D.M. acknowledge financial support of their work by Laboratoire d'Excellence Revive (Investissement d'Avenir, ANR-10-LABX-73). A.L.H. was supported by a postdoctoral fellowship from the Fondation pour la Recherche Médicale and a Marie Curie International Reintegration Grant (MC-IRG248496/SATELLITE CELL). The authors thank A. Vallée and D. Grégoire for help with tissue sectioning and assistance with the Apotome; C. Huret and D. Castel for advice and reagents for lentiviral production; and C. Rougeulle and N. Diguet for comments and discussions on the manuscript. They are grateful to S. Arbogast for advice on ROS quantification, to A. Lombes for advice and reagents on mitochondrial function, and to S. Yennek and S. Tajbakhsh for reagents.

Received: October 4, 2013
Revised: February 21, 2014
Accepted: April 3, 2014
Published: May 27, 2014

REFERENCES

Abbas, H.A., Maccio, D.R., Coskun, S., Jackson, J.G., Hazen, A.L., Sills, T.M., You, M.J., Hirschi, K.K., and Lozano, G. (2010). Mdm2 is required for survival of hematopoietic stem cells/progenitors via dampening of ROS-induced p53 activity. Cell Stem Cell *7*, 606–617.

Amendt, B.A., Sutherland, L.B., Semina, E.V., and Russo, A.F. (1998). The molecular basis of Rieger syndrome. Analysis of Pitx2 homeodomain protein activities. J. Biol. Chem. *273*, 20066–20072.

Babizhayev, M.A. (2012). Biomarkers and special features of oxidative stress in the anterior segment of the eye linked to lens cataract and the trabecular meshwork injury in primary open-angle glaucoma: challenges of dual combination therapy with N-acetylcarnosine lubricant eye drops and oral formulation of nonhydrolyzed carnosine. Fundam. Clin. Pharmacol. *26*, 86–117.

Beckers, J., Caron, A., Hrabé de Angelis, M., Hans, S., Campos-Ortega, J.A., and Gossler, A. (2000). Distinct regulatory elements direct delta1 expression in the nervous system and paraxial mesoderm of transgenic mice. Mech. Dev. *95*, 23–34.

Biressi, S., Tagliafico, E., Lamorte, G., Monteverde, S., Tenedini, E., Roncaglia, E., Ferrari, S., Ferrari, S., Cusella-De Angelis, M.G., Tajbakhsh, S., and Cossu, G. (2007). Intrinsic phenotypic diversity of embryonic and fetal myoblasts is revealed by genome-wide gene expression analysis on purified cells. Dev. Biol. *304*, 633–651.

Blanchet, E., Annicotte, J.S., Lagarrigue, S., Aguilar, V., Clapé, C., Chavey, C., Fritz, V., Casas, F., Apparailly, F., Auwerx, J., and Fajas, L. (2011). E2F transcription factor-1 regulates oxidative metabolism. Nat. Cell Biol. *13*, 1146–1152.

Bonner, W.M., Redon, C.E., Dickey, J.S., Nakamura, A.J., Sedelnikova, O.A., Solier, S., and Pommier, Y. (2008). GammaH2AX and cancer. Nat. Rev. Cancer *8*, 957–967.

Bourens, M., Fontanesi, F., Soto, I.C., Liu, J., and Barrientos, A. (2013). Redox and reactive oxygen species regulation of mitochondrial Cytochrome C oxidase biogenesis. Antioxid. Redox Signal *19*, 1940–1952.

Buckingham, M., and Vincent, S.D. (2009). Distinct and dynamic myogenic populations in the vertebrate embryo. Curr. Opin. Genet. Dev. *19*, 444–453.

Cao, H., Florez, S., Amen, M., Huynh, T., Skobe, Z., Baldini, A., and Amendt, B.A. (2010). Tbx1 regulates progenitor cell proliferation in the dental epithelium by modulating Pitx2 activation of p21. Dev. Biol. *347*, 289–300.

Coulon, V., L'Honoré, A., Ouimette, J.F., Dumontier, E., van den Munckhof, P., and Drouin, J. (2007). A muscle-specific promoter directs Pitx3 gene expression in skeletal muscle cells. J. Biol. Chem. *282*, 33192–33200.

Davis, R.L., Weintraub, H., and Lassar, A.B. (1987). Expression of a single transfected cDNA converts fibroblasts to myoblasts. Cell *51*, 987–1000.

Engleka, K.A., Gitler, A.D., Zhang, M., Zhou, D.D., High, F.A., and Epstein, J.A. (2005). Insertion of Cre into the Pax3 locus creates a new allele of Splotch and identifies unexpected Pax3 derivatives. Dev. Biol. *280*, 396–406.

Grégoire, D., and Kmita, M. (2008). Recombination between inverted loxP sites is cytotoxic for proliferating cells and provides a simple tool for conditional cell ablation. Proc. Natl. Acad. Sci. USA *105*, 14492–14496.

Griffith, O.W. (1982). Mechanism of action, metabolism, and toxicity of buthionine sulfoximine and its higher homologs, potent inhibitors of glutathione synthesis. J. Biol. Chem. *257*, 13704–13712.

Grifone, R., Demignon, J., Houbron, C., Souil, E., Niro, C., Seller, M.J., Hamard, G., and Maire, P. (2005). Six1 and Six4 homeoproteins are required for Pax3 and Mrf expression during myogenesis in the mouse embryo. Development *132*, 2235–2249.

Hutcheson, D.A., Zhao, J., Merrell, A., Haldar, M., and Kardon, G. (2009). Embryonic and fetal limb myogenic cells are derived from developmentally distinct progenitors and have different requirements for beta-catenin. Genes Dev. *23*, 997–1013.

Jacobs, F.M., Smits, S.M., Noorlander, C.W., von Oerthel, L., van der Linden, A.J., Burbach, J.P., and Smidt, M.P. (2007). Retinoic acid counteracts developmental defects in the substantia nigra caused by Pitx3 deficiency. Development *134*, 2673–2684.

Jean, E., Laoudj-Chenivesse, D., Notarnicola, C., Rouger, K., Serratrice, N., Bonnieu, A., Gay, S., Bacou, F., Duret, C., and Carnac, G. (2011). Aldehyde dehydrogenase activity promotes survival of human muscle precursor cells. J. Cell. Mol. Med. *15*, 119–133.

Jiang, Z., Liang, P., Leng, R., Guo, Z., Liu, Y., Liu, X., Bubnic, S., Keating, A., Murray, D., Goss, P., and Zacksenhaus, E. (2000). E2F1 and p53 are dispensable, whereas p21(Waf1/Cip1) cooperates with Rb to restrict endoreduplication and apoptosis during skeletal myogenesis. Dev. Biol. *227*, 8–41.

Karanjawala, Z.E., Murphy, N., Hinton, D.R., Hsieh, C.L., and Lieber, M.R. (2002). Oxygen metabolism causes chromosome breaks and is associated with the neuronal apoptosis observed in DNA double-strand break repair mutants. Curr. Biol. *12*, 397–402.

Kelly, D.P., and Scarpulla, R.C. (2004). Transcriptional regulatory circuits controlling mitochondrial biogenesis and function. Genes Dev. *18*, 357–368.

L'Honoré, A., Coulon, V., Marcil, A., Lebel, M., Lafrance-Vanasse, J., Gage, P., Camper, S., and Drouin, J. (2007). Sequential expression and redundancy of Pitx2 and Pitx3 genes during muscle development. Dev. Biol. *307*, 421–433.

L'honoré, A., Ouimette, J.F., Lavertu-Jolin, M., and Drouin, J. (2010). Pitx2 defines alternate pathways acting through MyoD during limb and somitic myogenesis. Development *137*, 3847–3856.

Lagha, M., Sato, T., Regnault, B., Cumano, A., Zuniga, A., Licht, J., Relaix, F., and Buckingham, M. (2010). Transcriptome analyses based on genetic screens for Pax3 myogenic targets in the mouse embryo. BMC Genomics *11*, 696.

Lee, S., Tak, E., Lee, J., Rashid, M.A., Murphy, M.P., Ha, J., and Kim, S.S. (2011). Mitochondrial H2O2 generated from electron transport chain complex I stimulates muscle differentiation. Cell Res. *21*, 817–834.

Lepper, C., Conway, S.J., and Fan, C.-M. (2009). Adult satellite cells and embryonic muscle progenitors have distinct genetic requirements. Nature *460*, 627–631.

Malinska, D., Kudin, A.P., Bejtka, M., and Kunz, W.S. (2012). Changes in mitochondrial reactive oxygen species synthesis during differentiation of skeletal muscle cells. Mitochondrion *12*, 144–148.

Messina, G., Biressi, S., Monteverde, S., Magli, A., Cassano, M., Perani, L., Roncaglia, E., Tagliafico, E., Starnes, L., Campbell, C.E., et al. (2010). Nfix regulates fetal-specific transcription in developing skeletal muscle. Cell *140*, 554–566.

Miniou, P., Tiziano, D., Frugier, T., Roblot, N., Le Meur, M., and Melki, J. (1999). Gene targeting restricted to mouse striated muscle lineage. Nucleic Acids Res. *27*, e27.

Montarras, D., Morgan, J., Collins, C., Relaix, F., Zaffran, S., Cumano, A., Partridge, T., and Buckingham, M. (2005). Direct isolation of satellite cells for skeletal muscle regeneration. Science *309*, 2064–2067.

Narciso, L., Fortini, P., Pajalunga, D., Franchitto, A., Liu, P., Degan, P., Frechet, M., Demple, B., Crescenzi, M., and Dogliotti, E. (2007). Terminally differentiated muscle cells are defective in base excision DNA repair and hypersensitive to oxygen injury. Proc. Natl. Acad. Sci. USA *104*, 17010–17015.

Navarro, P., Oldfield, A., Legoupi, J., Festuccia, N., Dubois, A., Attia, M., Schoorlemmer, J., Rougeulle, C., Chambers, I., and Avner, P. (2010). Molecular coupling of Tsix regulation and pluripotency. Nature *468*, 457–460.

Owusu-Ansah, E., and Banerjee, U. (2009). Reactive oxygen species prime Drosophila haematopoietic progenitors for differentiation. Nature *461*, 537–541.

Pallafacchina, G., François, S., Regnault, B., Czarny, B., Dive, V., Cumano, A., Montarras, D., and Buckingham, M. (2010). An adult tissue-specific stem cell in its niche: a gene profiling analysis of in vivo quiescent and activated muscle satellite cells. Stem Cell Res. (Amst.) *4*, 77–91.

Patti, M.E., Butte, A.J., Crunkhorn, S., Cusi, K., Berria, R., Kashyap, S., Miyazaki, Y., Kohane, I., Costello, M., Saccone, R., et al. (2003). Coordinated reduction of genes of oxidative metabolism in humans with insulin resistance and diabetes: Potential role of PGC1 and NRF1. Proc. Natl. Acad. Sci. USA *100*, 8466–8471.

Paylakhi, S.H., Fan, J.B., Mehrabian, M., Sadeghizadeh, M., Yazdani, S., Katanforoush, A., Kanavi, M.R., Ronaghi, M., and Elahi, E. (2011). Effect of PITX2 knockdown on transcriptome of primary human trabecular meshwork cell cultures. Mol. Vis. *17*, 1209–1221.

Puri, P.L., Bhakta, K., Wood, L.D., Costanzo, A., Zhu, J., and Wang, J.Y. (2002). A myogenic differentiation checkpoint activated by genotoxic stress. Nat. Genet. *32*, 585–593.

Relaix, F., Rocancourt, D., Mansouri, A., and Buckingham, M. (2005). A Pax3/Pax7-dependent population of skeletal muscle progenitor cells. Nature *435*, 948–953.

Relaix, F., Montarras, D., Zaffran, S., Gayraud-Morel, B., Rocancourt, D., Tajbakhsh, S., Mansouri, A., Cumano, A., and Buckingham, M. (2006). Pax3 and Pax7 have distinct and overlapping functions in adult muscle progenitor cells. J. Cell Biol. *172*, 91–102.

Remels, A.H., Langen, R.C., Schrauwen, P., Schaart, G., Schols, A.M., and Gosker, H.R. (2010). Regulation of mitochondrial biogenesis during myogenesis. Mol. Cell. Endocrinol. *315*, 113–120.

Richards, S.A., Muter, J., Ritchie, P., Lattanzi, G., and Hutchison, C.J. (2011). The accumulation of un-repairable DNA damage in laminopathy progeria fibroblasts is caused by ROS generation and is prevented by treatment with N-acetyl cysteine. Hum. Mol. Genet. 20, 3997–4004.

Satoh, J., Kawana, N., and Yamamoto, Y. (2013). Pathway analysis of ChIP-seq-based NRF1 target genes suggests a logical hypothesis of their involvement in the pathogenesis of neurodegenerative diseases. Gene Regul. Syst. Bio. 7, 139–152.

Semina, E.V., Reiter, R., Leysens, N.J., Alward, W.L., Small, K.W., Datson, N.A., Siegel-Bartelt, J., Bierke-Nelson, D., Bitoun, P., Zabel, B.U., et al. (1996). Cloning and characterization of a novel bicoid-related homeobox transcription factor gene, RIEG, involved in Rieger syndrome. Nat. Genet. *14*, 392–399.

Semina, E.V., Reiter, R.S., and Murray, J.C. (1997). Isolation of a new homeobox gene belonging to the Pitx/Rieg family: expression during lens development and mapping to the aphakia region on mouse chromosome 19. Hum. Mol. Genet. *6*, 2109–2116.

Sena, L.A., and Chandel, N.S. (2012). Physiological roles of mitochondrial reactive oxygen species. Mol. Cell *48*, 158–167.

Shiloh, Y. (2003). ATM and related protein kinases: safeguarding genome integrity. Nat. Rev. Cancer *3*, 155–168.

Takubo, K., Goda, N., Yamada, W., Iriuchishima, H., Ikeda, E., Kubota, Y., Shima, H., Johnson, R.S., Hirao, A., Suematsu, M., and Suda, T. (2010). Regulation of the HIF-1α level is essential for hematopoietic stem cells. Cell Stem Cell *7*, 391–402.

Ufer, C., and Wang, C.C. (2011). The roles of glutathione peroxidases during embryo development. Front. Mol. Neurosci. *4*, 12.

van den Munckhof, P., Luk, K.C., Ste-Marie, L., Montgomery, J., Blanchet, P.J., Sadikot, A.F., and Drouin, J. (2003). Pitx3 is required for motor activity and for survival of a subset of midbrain dopaminergic neurons. Development *130*, 2535–2542.

Varçin, M., Bentea, E., Mertens, B., Haute, C.V., Baekelandt, V., Michotte, Y., and Sarre, S. (2011). Acute versus long-term effects of 6-hydroxydopamine on oxidative stress and dopamine depletion in the striatum of mice. J. Neurosci. Methods *202*, 128–136.

Vasiliou, V., Pappa, A., and Estey, T. (2004). Role of human aldehyde dehydrogenases in endobiotic and xenobiotic metabolism. Drug Metab. Rev. *36*, 279–299.

Wei, Q., and Adelstein, R.S. (2002). Pitx2a expression alters actin-myosin cytoskeleton and migration of HeLa cells through Rho GTPase signaling. Mol. Biol. Cell *13*, 683–697.

Weintraub, H., Davis, R., Tapscott, S., Thayer, M., Krause, M., Benezra, R., Blackwell, T.K., Turner, D., Rupp, R., Hollenberg, S., et al. (1991). The myoD gene family: nodal point during specification of the muscle cell lineage. Science *251*, 761–766.

Zacksenhaus, E., Jiang, Z., Chung, D., Marth, J.D., Phillips, R.A., and Gallie, B.L. (1996). pRb controls proliferation, differentiation, and death of skeletal muscle cells and other lineages during embryogenesis. Genes Dev. *10*, 3051–3064.